Published in final edited form as:
Invest Ophthalmol Vis Sci. 2006 October ; 47(10): 4579–4588. doi:10.1167/iovs.06-0440.

Genomic Rearrangements of the *PRPF31* Gene Account for 2.5% of Autosomal Dominant Retinitis Pigmentosa

Lori S. Sullivan[1], **Sara J. Bowne**[1], **C. Robyn Seaman**[1], **Susan H. Blanton**[2], **Richard A. Lewis**[3,4], **John R. Heckenlively**[5], **David G. Birch**[6], **Dianna Hughbanks-Wheaton**[6], and **Stephen P. Daiger**[1,7]

[1] Human Genetics Center, The University of Texas Health Science Center at Houston, Texas

[7] Department of Ophthalmology and Visual Science, School of Public Health, The University of Texas Health Science Center at Houston, Texas

[2] Department of Pediatrics, University of Virginia, Charlottesville, Virginia

[3] Department of Ophthalmology, Cullen Eye Institute, Baylor College of Medicine, Houston, Texas

[4] Department of Molecular and Human Genetics, Cullen Eye Institute, Baylor College of Medicine, Houston, Texas

[5] Kellogg Eye Center, University of Michigan, Ann Arbor, Michigan

[6] The Retina Foundation of the Southwest, Dallas, Texas

Abstract

Purpose—To determine whether genomic rearrangements in the PRPF31 (RP11) gene are a frequent cause of autosomal dominant retinitis pigmentosa (adRP) in a cohort of patients with adRP.

Methods—In a cohort of 200 families with adRP, disease-causing mutations have previously been identified in 107 families. To determine the cause of disease in the remaining families, linkage testing was performed with markers for 13 known adRP loci. In a large American family, evidence was found of linkage to the *PRPF31* gene, although DNA sequencing revealed no mutations. SNP testing throughout the genomic region was used to determine whether any part of the gene was deleted. Aberrant segregation of a SNP near exon 1 was observed, leading to the testing of additional SNPs in the region. After identifying an insertion–deletion mutation, the remaining 92 families were screened for genomic rearrangements in *PRPF31* with multiplex ligation-dependent probe amplification (MLPA).

Results—Five unique rearrangements were identified in the 93 families tested. In the large family used for linkage exclusion testing, an insertion–deletion was found that disrupts exon 1. The other four mutations identified in the cohort were deletions, ranging from 5 kb to greater than 45 kb. Two of the large deletions encompass all PRPF31 as well as several adjacent genes. The two smaller deletions involve either 5 or 10 completely deleted exons.

Conclusions—In an earlier long-term study of 200 families with adRP, disease-causing mutations were identified in 53% of the families. Mutation-testing by sequencing missed large-scale genomic rearrangements such as insertions or deletions. MLPA was used to identify genomic rearrangements

Corresponding author: Lori S. Sullivan, Human Genetics Center, School of Public Health, The University of Texas Health Science Center at Houston, 1200 Herman Pressler, Houston, TX 77030; lori.s.sullivan@uth.tmc.edu.

Disclosure: **L.S. Sullivan**, None; **S.J. Bowne**, None; **C.R. Seaman**, None; **S.H. Blanton**, None; **R.A. Lewis**, None; **J.R. Heckenlively**, None; **D.G. Birch**, None; **D. Hughbanks-Wheaton**, None; **S.P. Daiger**, None

in *PRPF31* in five families, suggesting a frequency of approximately 2.5%. Mutations in PRPF31 now account for 8% of this adRP cohort.

Retinitis pigmentosa (RP) is the most common form of inherited retinopathy, with a prevalence of approximately 1 in 3500.[1] From linkage mapping, positional cloning, and candidate gene screening, at least 35 unique loci have been identified for nonsyndromic forms of RP. The underlying genes for 26 of these loci have been reported (RetNet; http//sph.uth.tmc.edu/RetNet/provided in the public domain by the University of Texas Houston Health Science Center, Houston, TX). For autosomal dominant (ad)RP, which accounts for 20% to 40% of all cases, 14 genes have been identified: *CA4*, *CRX*, *FSCN2*, *GUCA1B*, *IMPDH1*, *NRL*, *PRPF3*, *PRPF8*, *PRPF31*, *RDS*, *RHO*, *ROM1*, *RP1*, and *RP9*. An additional locus, *RP31*, has also been mapped recently.[2]

In a series of ongoing studies, we selected a set of 200 families with a clinical diagnosis and pedigree evidence of adRP. Our criteria were either (1) the presence of affected individuals in three or more generations, with both males and females among all affected family members, or (2) at least two affected generations with male-to-male transmission. The requirements for three generations, including females, or for male-to-male transmission, reduced the likelihood of including X-linked families.

A mutation-screening survey of the 200 families in this adRP cohort was reported recently.[3] We screened the complete coding regions of *CA4*, *CRX*, *FSCN2*, *IMPDH1*, *NRL*, *PRPF31*, *RDS*, *RHO*, *ROM1*, and *RP9*, as well as mutation hotspots in *RP1*, *PRPF3*, and *PRPF8*. *GUCA1B* was not tested because it is a rare cause of adRP, if a cause at all.[4] In several families with no male-to-male transmission, we also screened portions of *RPGR*. As a result of this screening, the likely disease-causing mutations were identified in 53% of the families.

What is the cause of disease in the 47% of patients in whom we cannot identify a disease-causing mutation? One possibility is that additional genes that can cause adRP have not been identified yet. Several lines of evidence suggest this is true, including several families in which linkage testing has excluded all known loci (Sullivan LS, et al. *IOVS* 2005;46:ARVO E-Abstract 2293). Another possibility is that known disease-causing genes harbor mutations that cannot be identified with standard screening techniques. Mutation screening is typically performed by PCR amplification of coding exons with primers located in the flanking introns. This allows detection of base substitutions and small insertions and deletions but misses other types of mutations. Large insertions, deletions, or genomic rearrangements prevent PCR amplification of the mutant allele, making such mutations invisible by sequencing. Mutations that affect splicing or expression are also likely to be missed.

Until recently, screening for genomic rearrangements was relatively difficult, requiring labor-intensive techniques, such as Southern hybridization, or low-resolution techniques, such as fluorescence in situ hybridization (FISH). Multiplex ligation-dependent probe amplification (MLPA) is a recently developed technique for the relative quantification of multiple nucleic acid sequences in one reaction.[5] With MLPA, up to 40 different specific target sequences can be detected and quantified in parallel.

MLPA probes consist of two oligonucleotides (half-probes) that are ligated by a heat-stable ligase, provided that both oligonucleotides are annealed to adjacent sites on a target sequence. Ligation products can be amplified simultaneously with the use of a single primer pair and yield an amplification product of unique size, between 90 and 500 bp. If one or both of the half-probes fail to hybridize, no amplification will occur. The copy number of the target sequences is reflected in the relative intensities of probe amplification products. Probe amplification products can be separated and quantified with a capillary electrophoresis system (Fig. 1).

MLPA detects deletions, duplications, and some base substitutions in the sequences to which the probes hybridize. Relatively little DNA is required, and several sites can be probed simultaneously. Although pre-made probe sets are available for various genes, custom probes are easily designed to fit specialized testing needs.

We used the *PRPF31* gene as a test of the MLPA technology, to determine its usefulness to detect large-scale alterations in adRP genes. PRPF31 encodes a protein involved in pre-mRNA splicing and mutations in PRPF31 were identified as a cause of adRP in 2001.[6] Our survey of adRP families suggested that it is the third most common cause of adRP, at ~6% of cases.[3] The gene has 13 coding exons and encodes a protein of 499 amino acids. Families that carry disease-causing mutations in PRPF31 often show incomplete penetrance, with numerous examples of obligate carriers having no clinical symptoms or signs.[6–9] The disease mechanism is likely to be haploinsufficiency,[10] with overexpression of the wild-type allele in asymptomatic carriers providing a protective effect.[9,11]

Methods

AdRP Cohort

The cohort of patients with adRP used in this study is described in detail elsewhere.[3] Briefly, this set of 200 families had a high likelihood of having the autosomal dominant form of retinitis pigmentosa. Each proband had been screened previously for mutations in the complete coding regions of *CA4*, *CRX*, *FSCN2*, *IMPDH1*, *NRL*, *PRPF31*, *RDS*, *RHO*, *ROM1*, and *RP9* and in mutation hotspots of *RP1*, *PRPF3*, and *PRPF8*. Of the 200 families in the cohort, likely disease-causing mutations have been identified in 107 families[3]; the remaining 93 families were tested in this study.

This study was performed in accordance with the Declaration of Helsinki, and informed consent was obtained from all participants. The research was approved by the Committee for Protection of Human Subjects, University of Texas, Houston, and by the respective human subjects review boards at each participating academic institution.

Linkage Exclusion

One family in the cohort, BCMAD014, was large enough to screen by "linkage exclusion." Linkage exclusion is linkage testing with markers tightly linked to a target locus. It is performed in families large enough to exclude linkage to most unlinked loci, but not necessarily large enough to confirm linkage to a linked locus. Linkage-exclusion testing is undertaken before a genome-wide linkage study, to assure that one of the known adRP loci is not the cause of disease.

Thirty-one DNA samples were available, 15 from affected individuals or obligate carriers and 16 from apparently unaffected individuals. A total of 33 STR markers flanking and/or within each of 13 adRP loci (*CRX*, *FSCN2*, *GUCA1B*, *IMPDH1*, *NRL*, *PRPF3*, *PRPF8*, *PRPF31*, *RDS*, *RHO*, *ROM1*, *RP1*, and *RP9*) were tested (Table 1). Five additional markers for the X-linked genes *RP2* and *RPGR* were also tested, because there was no observed male-to-male transmission in the family.

STR loci were amplified from patient DNAs with fluorescent PCR primers and DNA polymerase (Ampli*Taq* Gold; Applied Biosystems [ABI], Foster City, CA; or HotStar*Taq* DNA polymerase (Qiagen, Valencia, CA), and standard multiplex reaction conditions. PCR products were pooled and diluted in water, added to deionized formamide (ABI) containing size standards (GeneScan-500 LIZ; ABI), and run on a genetic analyzer (model 3100-Avant; ABI). Genotype data were then analyzed (GeneMapper version 3.7; ABI). Two-point and

multipoint linkage analysis was performed with version 5.1 of the LINKAGE package,[12] using a dominant model with 90% penetrance.

SNP Testing and DNA Sequencing

From the SNP database, we chose 17 SNPs that spanned the 16-kb region containing the *PRPF31* gene and had high heterozygosity values. Primers were designed to amplify and sequence each of the 17 SNPs shown in Table 2. PCR amplification and sequencing were performed as previously described.[3] In general, 30 to 50 ng of genomic DNA was amplified (Ampli*Taq* Gold; ABI; or HotStarTaq; Qiagen) in a 12.5-μL reaction volume for 35 cycles. PCR products were treated with an enzyme cleanup solution (ExoSapIt; USB, Cleveland, OH) and sequenced bidirectionally with dye termination chemistry (BigDye v1.1; ABI). Sequence reactions were purified with Sephadex columns (Princeton Separations, Adelphia, NJ) and run on a genetic analyzer (model 3100-Avant; ABI). Sequence analysis was performed on computer (SeqScape software; ABI).

Twelve related individuals from family BCMAD014 were genotyped for each SNP, and the results were analyzed to identify SNPs with an abnormal segregation pattern (Fig. 2). Additional SNP markers were tested subsequently, to refine the hemizygous region. Primers flanking the deleted region were used for amplification and sequencing of affected individuals, to determine the exact nature of the insertion–deletion mutation.

Multiplex Ligation-Dependent Probe Amplification

Probes—Twenty-one probe pairs were designed initially for the RP11 gene: two to detect specifically the indel found in the BCMAD014 family, one located in the promoter region, and the rest designed to cover the sites of our existing set of amplification–sequencing primers, located in the flanking introns.[3] Probes ranged in size from 97 to 145 bp, with half-probe sizes from 44 to 79 nucleotides in length (Table 3A; additional details online in Supplementary Table S1, http://www.iovs.org/cgi/content/full/47/10/4579/DC1). Although the 21 probes were designed to have nonoverlapping sizes, probe signals were not always well resolved. To solve this problem, we split the probes into two testing panels: set D with 14 probes (which was run in combination with the P115 Retina kit), and set X with 7 probes (run in combination with 10 synthetic probes for additional genes).

For probe design, we followed the recommendations of Stern et al.[13] and MRC-Holland (Amsterdam, The Netherlands). Each 5′ or 3′ half-probe contains a unique target sequence linked to universal primer sequences at their 5′ or 3′ ends, respectively (Table 3; Supplementary Table S1, http://www.iovs.org/cgi/content/full/47/10/4579/DC1; Fig. 1). The hybridizing portion of the probe was chosen to have an annealing temperature of >65°C, calculated with the program Raw-Probe (MRC-Holland). Target sequences were screened for the presence of SNPs that would affect probe binding and for the presence of repeat sequences that would affect specificity. All primers were synthesized by Integrated DNA Technologies (IDT, Coralville, IA) and were desalted at the time of synthesis, but underwent no additional purification. Each 3′ half-probe was synthesized with a 5′ phosphate group necessary for probe ligation.

A set of 13 external probes, extending 27 kb upstream from the start of *PRPF31* and 29 kb downstream from the end of *PRPF31* were designed to map the large deletions found in families UTAD119 and UTAD034 (Table 3B; Supplementary Table S1, http://www.iovs.org/cgi/content/full/47/10/4579/DC1). Five upstream probes are located within the exons of three genes: *OSCAR*, *NDUFA3*, and *TFPT*. Six downstream probes are located within the exons of three other genes: *CNOT3*, *LENG1*, and *TMC4* (Fig. 3B; Supplementary Table S1 online). For mapping deletions internal to PRPF31, three probes were

made within intron 3, and one was made in intron 8 (Table 3C; Supplementary Table S1 online; Fig. 3A). The external and internal probes were also split into two testing panels, A and B.

MLPA Reaction—MLPA reactions were performed with the reagents in either one of two kits (MLPA P115 Retina or EK1 kit; MRC-Holland) and the manufacturer's DNA detection–quantification protocol. Synthetic probe cocktails corresponding to each custom *PRPF31* panel were created by combining and diluting primers to an individual concentration of 0.4 to 4.0 nM. Optimal primer concentrations were determined experimentally, to best equalize the peak heights from each probe set in a given panel.

Probe cocktails were hybridized overnight at 60°C with 50 ng of genomic DNA. Hybridized probes were ligated for 15 minutes at 54°C, followed by 5 minutes at 98°C. One-fourth of the ligation reaction was used for amplification, according to the manufacturer's protocol, with universal 5′ *N*-(3-fluoranthyl)maleimide (FAM)-labeled primer (GGGTTCCCTAAGGGTTGGA) and the 3′ primer (TCTAGATTGGATCTTGCTGGCAC). Alternately, the volume of the PCR reaction was reduced to 25-μL, and only 5μL of the ligation reaction was used as a template. One microliter of PCR product was diluted in deionized formamide (ABI) containing size standards (GeneScan-500 LIZ; ABI) and run on a genetic analyzer (model 3100-Avant; ABI). Additional testing was performed on samples with decreased signal from one or more probes.

MLPA Data Analysis—Preliminary analysis of the products was performed with mapping software (GeneMapper 3.7; ABI). Tables from the software containing data on peak heights and peak areas were exported to a spreadsheet (Excel; Microsoft, Redmond, WA).

Calculation of probe copy numbers was based on Stern et al.[13] First, probe normalization was performed on each sample by summing the raw peak areas of all the control probes, followed by dividing each of the raw peak areas by the sum of the control probe areas. Then, to minimize sample variation, the normalized peak areas for each probe were averaged across the three control samples. Finally, the normalized peak areas of the test samples were divided by the averaged normalized peak areas of the control samples, to produce a ratio of test probe to control probe. This ratio is called the dosage quotient (DQ). A DQ of 1.0 indicates the presence of two alleles and 0.5 or 1.5 suggests either deletion or duplication of the target sequence, respectively.

Results

Our cohort of 200 adRP families was screened previously for mutations by conventional sequencing strategies. This led us to the underlying mutation(s) responsible for disease in 107 families.[3] Our efforts are now focused on the remaining 93 families. We believe that these families represent two categories: one set with mutations in known genes that were not detected by sequencing and another with mutations in genes that have not been identified yet. If the families are big enough and enough DNA samples are available, we can rule out the first possibility through linkage exclusion testing to the known adRP loci. Conversely, if a family shows linkage to a known gene that we have screened already, we must reevaluate the screening.

Family BCMAD014

This family in our adRP cohort was a likely candidate for a *PRPF31* mutation. A large multigenerational pedigree was available, and it showed multiple occurrences of apparent incomplete penetrance, a hallmark of many *RP11* families.[7,8] Screening of the 13 coding exons by DNA sequencing revealed no obvious disease-causing mutations. Linkage testing to markers for *PRPF31* showed strong evidence of linkage, producing a multipoint lod score >3.0.

The other 12 adRP loci were either excluded definitively or were uninformative, suggesting that *PRPF31* is the most likely candidate (Table 1). We tested several SNPs across the *PRPF31* region in 12 family members, looking for evidence of abnormal segregation that might indicate a deletion.

SNP rs4806711, located 14 bp past the end of exon 1 (a noncoding exon), showed an abnormal pattern consistent with allelic dropout of the affected allele (Fig. 2). A SNP 1.6 kb upstream from exon 1 showed normal segregation, as did SNPs from exons 3 through 14, limiting the region of interest. All published SNPs from the region were tested subsequently, and the entire region was sequenced completely, to identify additional polymorphisms. Only the original SNP, rs4806711, showed aberrant segregation. Testing of additional markers reduced the possible hemizygous region to approximately 1200 bp. We used PCR primers flanking this region to amplify and sequence across the presumed deletion. Sequencing revealed a complex insertion–deletion (indel): a deletion of 110 bp of exon 1+39 bp of intron 1+insertion of 640 bp. The origin of the 640-bp insertion appears to be the *OSCAR* gene, which is located 20 kb 5′ to *PRPF31*. SNP rs4806711 and one of the primers used to amplify it are within the deleted region, making carriers hemizygous for this SNP. Amplification across the indel, with flanking primers, shows that in all cases the indel cosegregates with disease.

Identification of the indel in BCMAD014 led us to speculate that genomic rearrangements may be a common cause of adRP, at least in genes such as *PRPF31* where haploinsufficiency is the likeliest disease mechanism. We decided to use MLPA to confirm the indel in BCMAD014 and to screen the remaining families in the cohort.

MLPA can be performed with prepackaged probe sets obtained from MRC-Holland or by synthesizing unique probes.[13,14] Because this study involved a novel MLPA target, without a preexisting probe set, all RP11 probes were designed in-house. In many cases we combined our synthetic probes with a kit (P115 Retina Kit; MRC-Holland) that includes 16 probes for rhodopsin, *RPE65*, and *RP1*, as well as 9 control probes.

We used MPLA to confirm the presence of the indel in BCMAD014. Two probes were designed: one located completely within the deleted region of exon 1 and intron 1, the other probe spanning the junction of deleted and retained sequence. We found that the probe that crosses the deletion–insertion site was present at only 50% levels in affected and carrier individuals from BCMAD014 (Fig. 3C). An unexpected finding was that the probe that is located entirely within the deleted sequence did not appear to be reduced, suggesting that as a result of the insertion–deletion event, the deleted DNA was inserted elsewhere in the genome and could still be detected by MLPA.

MLPA of *PRPF31* in the adRP Cohort

After confirming the indel in BCMAD014, we next screened the entire *PRPF31* gene in the 93 families in the adRP cohort without identifiable mutations in other adRP genes. We used a set of 21 MLPA probes that were designed to detect changes in the sequences in which we routinely place our PCR primers. In these 93 families we found 7 probands with at least one PRPF31 probe with a DQ of 0.6 or less, suggesting hemizygosity at that probe site. Three families had identical rearrangements—BCMAD014, RFS178, and UTAD305—and ultimately could be joined in a single pedigree. For statistical purposes, we count this as a single mutation and note that it reduced the size of the adRP cohort to 198 families. The four remaining families each had unique mutations: two within the *PRPF31* gene and two encompassing the whole gene and extending beyond (Table 4).

BCMAD014, RFS178, and UTAD305—Two families, not previously known to be related, showed the heterozygous loss of the exon 1 probe that was designed to detect the indel found

in BCMAD014 (Fig. 3C). On careful inspection of each family's pedigree, we discovered that all three probands were related and represented a single family. We tested 13 affected family members and 2 obligate carriers; all had the exon 1 indel. This mutation is expected to disrupt mRNA splicing of exon 1 to exon 2 and thus to prevent protein production from the mutant allele.

UTAD069—The proband from this family showed the heterozygous deletion of eight probes from the set of 21 covering exons 1 through 14 of *PRPF31*. The first deleted probe is 5′ of exon 4 and the last deleted probe is 3′ of exon 8 (Figs. 3A, 3D). All probes in between have DQs of ~0.40 to 0.59, suggesting the complete deletion of exons 4 through 8. Four additional probes were designed to refine the mapping: three in the intron between exons 3 and 4, and 1 in the intron between exons 8 and 9. Only the probe 960 bp in front of exon 4 had a DQ of <1, placing the deletion breakpoints between 0.96 and 1.3 kb in front of exon 4 and <1 kb past exon 8. PCR amplification across the deletion was performed to determine the actual breakpoints, and a deletion of 4843 bp was observed. Both breakpoints are located in Alu repeats. No additional family members were available for testing.

UTAD082—The proband of this family showed heterozygous deletion of 14 of the 21 probes from *PRPF31*. The first deleted probe is 5′ of exon 4, and the last deleted probe is 3′ of exon 13. All probes between had DQs ranging from ~0.51 to 0.68, suggesting the complete deletion of exons 4 through 13. The three probes located in the intron between exons 3 and 4 were also tested, and all three were found to be deleted. This places the 5′ deletion breakpoint >2 kb upstream from the start of exon 4 (in a different spot than that in UTAD069; Figs. 3A, 3E). The 3′ breakpoint is within the 2-kb intron between exons 13 and 14 and was not refined further by MLPA. Three additional affected family members and one obligate carrier were tested with the entire panel of *PRPF31* probes. All showed heterozygous deletion of exons 4 through 13.

The MLPA data suggest a deletion of at least 9.7 kb, with a maximum possible size of 12.4 kb. PCR primers in introns 3 and 13 were used to amplify and sequence the region, to confirm the deletion and determine its boundaries. As expected, the deletion encompasses exons 4 through 13 and has a total size of 11.2 kb. Both the breakpoint in intron 3 and the breakpoint in intron 13 occur at equivalent positions in nearly identical AluY repeats.

UTAD119—The proband of this family showed the heterozygous deletion of all 21 *PRPF31* probes (Figs. 3A, 3F). An additional set of 13 MLPA probes, extending 27 kb upstream and 29 kb downstream of *PRPF31*, was tested to determine the size of the deletion (Table 3B, Fig. 3B). Results from these probes showed that the deletion extends at least 15 kb upstream from *PRPF31*, encompassing the genes *NDUFA3* and *TFPT*. The *OSCAR* gene is likely to be only partially deleted, with the MLPA probe located in exon 1 deleted but the probe in exon 5 appearing normal. On the other side of *PRPF31*, the deletion extends a relatively small distance from the end of the gene, with the probe located 1.5 kb from the end deleted, whereas the probes at 6 kb and beyond are normal (Fig. 3B). Based on these results, the estimated size of the deletion is 32 to 42 kb. No additional family members were available for testing

UTAD034—All 21 *PRPF31* probes were also heterozygously deleted in this family (Figs. 3A, Fig. 3G). The panel of 13 external probes was tested and showed that the deletion is at least 44.8 kb. A minimum of 27 kb of the upstream sequence is missing, with all six probes showing DQs of <0.6. This encompasses *TFPT*, *NDUFA3*, and *OSCAR*. Downstream, the probe located 1.5 kb from the end of *PRPF31* is deleted, whereas the more distant probes appeared normal. Only a single affected individual was available for testing.

MLPA of Rhodopsin, *RP1*, and *RPE65*

All members of the cohort were screened with the MLPA kit (P115 Retina kit; MRC-Holland) and the set of *PRPF31* probes. This kit includes probes for rhodopsin, *RP1*, and *RPE65*, and control probes. All samples appeared to have normal DQs for these retinal gene probes, and no heterozygous deletions were detected.

Phenotypic Description of Families with Genomic Rearrangements

BCMAD014—This family of Scottish and English ancestry emigrated to South Carolina in the mid-19th century and migrated to central Texas by the turn of the century. When examined in 1984 at a family reunion, at least four living generations had affected individuals; males were as severely affected as females. The onset of symptoms was typically in the first decade of life, usually between ages 5 and 9 years. A few individuals presented later for diagnosis, but the age of retrospective complaints of poor vision in dim light and poor adaptation to bright light was earlier than midteens. By the fifth decade, all affected individuals had no useful vision (<20/400), many had classic posterior cortical stellate cataracts or had had cataract surgery, and most had advanced geographic macular atrophy and/or severely constricted visual fields (<5° in all meridians), in concert with vascular narrowing, classic pigmentary retinopathy with bone spicules densely in the peripheral retinas of each eye, and pallor of the optic discs. At least three individuals were obligate gene carriers by position in the pedigree, yet showed no clinical phenotype when examined at ages 53, 43, and 39 years (electrophysiology was not performed). Except for scattered reports of late adult-onset hearing impairment, occasional speech deficits, and two instances of renal stones (none of which seems to segregate with the retinitis pigmentosa), no other medical history was reported during questioning of the subjects at the initial examination or in subsequent discussions in 2004.

UTAD069—The proband was first seen in 1981 at age 46 with a history of noting visual field loss since age 5 and night blindness since the early teenage years. There was a four-generation history of RP in her family. Wearing a −7.00 correction for myopia, she had visual acuity of OD: 20/60, OS: 20/50. She had a trace posterior subcapsular cataract in both eyes on slit lamp examination and a moderate pigmentary retinopathy on fundus examination. Her electroretinogram (ERG) was nonrecordable under all conditions. Goldmann visual fields showed advanced disease with contracted central fields: The 1-mm target was 2° OU, whereas the 4 mm target was OD 7° and OS 9°. By 1988, her visual acuity had decreased to OD 5/200, OS handmotion vision, with Goldmann visual fields of OD 3°, OS 1° with 4-mm targets.

UTAD082—Three individuals were examined in this family. The proband was first seen in 1979 at age 22. Her family history showed at least three generations of affected individuals, with her father having no symptoms, but his brother and mother were affected. Her father had four daughters, all of whom were affected. The proband had a history of night blindness from early childhood. Her visual acuity was 20/20 OU with correction. Fundus examination showed a pigmentary retinopathy. Goldmann visual fields with a 4-mm target were relatively full, whereas the 1-mm target demonstrated contracted fields OD: 6°, OS: 8°. The ERG was nonrecordable under all conditions. When she returned in 1998, her visual acuity was OD: 20/70, OS: 20/40, with correction. She had central fields, and with the 4-mm target they showed OD: 12°, OS: 13°, whereas the 1-mm target showed 5° in both eyes.

The proband's younger sister was seen in 1979 at age 15. At that time, her complaint was peripheral vision loss, but she denied night blindness. Her ERG at age 22 showed photopic ERG with normal amplitudes of OD: 137 μV, and OS: 145 μV, but very abnormal implicit times at OD: 40 ms, OS: 39 ms (normal, 32 ± 1 ms). The rod isolate ERG was nonrecordable, whereas bright-flash, dark-adapted responses were abnormal with b-wave amplitudes approximately 25% of normal. Goldmann visual fields were normal with larger isopters, but

the 1 mm showed some contraction at OD: 39°, OS: 41°. She was seen again in 1993, at which time her vision was the same, and her visual fields slightly contracted from before. Fundus examination showed diffuse retinal atrophy of equatorial regions with bone spiculelike pigment deposits.

Another affected sister was evaluated in 1981, at which time she stated she had had night blindness her entire life, but had not noted visual field defects. Her visual acuity was 20/20 OU with correction. Her ERG showed a rod–cone degeneration pattern with a nonrecordable rod-isolated ERG, whereas the photopic ERG b-wave was approximately 65% of normal. The bright-flash, dark-adapted ERG was proportionately worse with b-wave amplitudes approximately 15% of normal. Fundus examination demonstrated diffuse retinal atrophy with bone spiculelike pigment deposits. In 1981, the Goldmann visual fields with the 1-mm target showed OD: 38°, OS: 36°, whereas the 4-mm target showed OD: 59°, OS: 59°. By 1993, her visual acuity was 20/25 OU with correction, and her visual fields showed with the 1-mm target, OD: 8°, OS: 7°, and with the 4-mm target, OD: 48°, OS: 45°. By age 44, her visual fields were reduced to <10° with the 4-mm target. On fundus photographs, all three sisters had optic nervehead drusen with a white ring at the edge of the optic nervehead.

UTAD119—Two members of this family have been examined. The proband was first evaluated in 1979 at age 16 at which time she reported night blindness. A family history suggested a four generation autosomal dominant form of disease with incomplete penetrance. Her visual acuity was 20/40 OU with correction. Posterior subcapsular cataracts were removed in 1982, which improved her vision from 20/80 to 20/40. An ERG performed in 1983 was nonrecordable under all conditions. Her first Goldmann visual field in 1979 showed a 9° central field with a 1-mm target OU. A 4-mm target was OD: 36°, OS: 47°. By 1999, her visual acuity was OD 20/25+ with contact lens and 20/30 OS with an intraocular lens. Her visual fields with the 1-mm target were OD: 5°, OS: 5°, and with the 4-mm target, OD: 10°, OS: 12°. This pattern is typical of a patient with rod–cone dystrophy, with preservation of central cone function.

The father of the proband was first seen in 1983 because of his daughter's diagnosis, although the father himself reported no symptoms. His general health was good. His visual acuity was 20/20 with correction OU. On fundus examination he had an early pigmentary retinopathy. His standardized ERG demonstrated a rod–cone pattern of loss with a photopic ERG approximately 25% of normal, whereas the rod-isolated ERG was nonrecordable. The bright-flash, dark-adapted ERG was barely recordable. The final rod threshold was 2.3 log units elevated at 20° above fixation. Goldmann visual fields showed full isopters with a 4-mm target, whereas with the 1-mm target, they were contracted to OD: 15°, OS: 23°. The patient was last seen in 1999, at which time he stated that he had had little change in his vision. He had developed ring scotomata in both eyes, and his Goldmann fields with a 1-mm target was OD: 7°, OS: 8°.

UTAD034—This man was first examined at age 15. He had come to medical attention at age 7 because of his paternal history of retinitis pigmentosa. His father had been functionally blind most of his adolescent life and had never driven an automobile. The paternal diagnosis of retinitis pigmentosa had been established by adolescence and was far advanced. No antecedent family history suggestive of retinitis pigmentosa was known, although his father was 33 at the time of the son's birth.

At age 7 years, the proband's ERGs were deemed "moderately to severely abnormal," based on prior medical records. At age 15, his best corrected visual acuity was 20/20, Jaeger 1, in each eye, with a moderate compound myopic refractive error (OD: −13.75 + 1.50 × 101; OS: −4.00 + 1.00 × 76). The results of the anterior segment and biomicroscopic examination of each eye were normal. Mild syneresis with 2+ cells was present in each vitreous cavity. The peripheral retinal pigment epithelium was atrophic, the peripheral retinal vasculature was

attenuated, and fine bone spicules were present in the peripheral retina. Minimal intrapapillary drusen were accompanied by moderate cystoid macular edema in each eye. Formal visual fields were constricted to <20° in all meridians with a ring spared in the periphery of each field. His cystoid macular edema responded well to weight-based doses of acetazolamide for the ensuing 19 years.

By age 24, posterior subcapsular shagreen had appeared in each lens, evolving within 2 years to typical posterior cortical cataracta complicata, reducing acuity to 20/40 in each eye, worsened by glare to 20/100 OD and 20/60 OS. Uncomplicated cataract surgery by phacoemulsification and posterior chamber pseudophakos implantation yielded 20/20 acuity centrally, associated with visual fields of <10° in all meridians. The retinal features of vascular attenuation and bone spicule formation became more prominent over the years, but the intrapapillary drusen did not change. He is a college graduate with an advanced degree. His general medical health is excellent except for a single bout with kidney stones of unknown type (not clearly related to the acetazolamide therapy).

Summary

The clinical phenotypes observed in the five families ranged from lack of penetrance (or mild symptoms late in life) to significant visual impairment and night blindness by age 20. Rod–cone dystrophy was often observed, and secondary cataracts had occurred on occasion. Lack of penetrance or very mild symptoms was observed in up to 10% of individuals with one of the *PRPF31* rearrangements. This constellation of symptoms is typical of retinal disease caused by missense and nonsense mutations in *PRPF31*, suggesting that the phenotype arising from haploinsufficiency is not qualitatively different. Hemizygous deletion of flanking genes, as is the case for two of the rearrangements, is not associated with obvious clinical findings, though subtle consequences cannot be excluded.

DISCUSSION

Although 14 genes that can cause autosomal dominant RP are currently known, mutations in these genes are found only in approximately half of patients with adRP. Although additional causal genes have not been identified yet, our present study suggests that we may be missing a substantial fraction of mutations by limiting our screening to DNA sequencing-based techniques. While sequencing detects small insertions or deletions located between PCR primers, sequencing alone does not detect rearrangements that disrupt PCR primer binding.

MLPA is one of several techniques available to detect genomic aberrations in copy number. Its major advantages are ease of use, high throughput, and the requirement for relatively small quantities of DNA.[5] Other techniques, such as quantitative real-time PCR, are more expensive, less sensitive, and lack the capacity for multiplexing of probes.[15]

Because we had already screened the coding exons by sequencing, our goal was to look for changes that might have affected the PCR amplification step of mutation screening. This required placing our primary set of *PRPF31* MLPA probes on top of sites where our PCR primers are located, usually in the flanking intronic sequence near intron–exon boundaries. We also placed a probe in a possible promoter region, upstream of the transcription start site.

Using MLPA and other techniques, we identified five novel genomic rearrangements in the *PRPF31* gene that cause retinitis pigmentosa. None of these mutations could have been detected by our standard sequencing-based screening protocol. The first mutation is an indel that disrupts the exon 1–intron 1 junction, almost certainly destroying any chance of correct mRNA splicing. The other four mutations are deletions of varying sizes. Two deletions are internal to the gene, removing either 5 or 10 coding exons. The other two deletions found in

the cohort are considerably larger, encompassing the entire *PRPF31* gene and at least three additional nearby genes.

The larger internal deletion, found in UTAD082, appears to have been caused by unequal homologous recombination between nearly identical AluY repeats. The deletion in UTAD069 may also involve a similar mechanism, as both breakpoints are in similar AluJo and AluSx repeats. This type of mechanism is predicted to cause 0.3% of human genetic diseases.[16] A total of 11 Alu repeats can be found within the introns of the *PRPF31* gene, providing ample opportunity for internal recombination.

All the mutations found in this screening are likely to cause RP by haploinsufficiency, in which one copy of the *PRPF31* gene is either disabled or totally gone. This is consistent with recent reports of novel *PRPF31* mutations[10] and with the analyses of gene expression in carriers of *PRPF31* mutations.[9,11] Several other genes are known to cause retinal degeneration through haploinsufficiency, such as peripherin/*RDS* and *FSCN2*, and these may also be likely candidates to have undetected deletions.

Clearly, we must move beyond simple sequencing when screening for disease-associated mutations. A recent report comparing sequencing alone to a combination of other techniques including MLPA, demonstrated that a substantial fraction of mutations in four breast cancer genes were missed by traditional screening methods[17]: seventeen percent of patients screened by sequencing had undetected genomic rearrangements that caused disease. Other recent papers have described similar outcomes, in which large genomic rearrangements account for a much higher proportion of deleterious mutations than previously appreciated.[18–20] MLPA is an effective tool to detect such mutations and a useful addition to our adRP screening protocols.

Supplementary Material

Refer to Web version on PubMed Central for supplementary material.

Acknowledgments

The authors thank the many families and patients who participated in this study and Elizabeth Cadena, Catherine Spellicy, and Jingya Zhu for technical assistance.

Supported by grants from the Foundation Fighting Blindness, the William Stamps Farish Fund, the Gustavus and Louise Pfeiffer Research Foundation, and the Hermann Eye Fund, and National Eye Institute Grants EY07142 and EY05235. RAL is a Senior Scientific Investigator of Research to Prevent Blindness, New York, which contributed unrestricted funds to these investigations.

References

1. Haim M. Epidemiology of retinitis pigmentosa in Denmark. Acta Ophthalmol Scand Suppl 2002;233:1–34. [PubMed: 11921605]
2. Papaioannou M, Chakarova CF, Prescott de QC, et al. A new locus (RP31) for autosomal dominant retinitis pigmentosa maps to chromosome 9p. Hum Genet 2005;118:501–503. [PubMed: 16189705]
3. Sullivan LS, Bowne SJ, Birch DG, et al. Prevalence of disease-causing mutations in families with autosomal dominant retinitis pigmentosa (adRP): a screen of known genes in 200 families. Invest Ophthalmol Vis Sci 2006;47:3052–3064. [PubMed: 16799052]
4. Payne AM, Downes SM, Bessant DA, et al. Genetic analysis of the guanylate cyclase activator 1B (GUCA1B) gene in patients with autosomal dominant retinal dystrophies. J Med Genet 1999;36:691–693. [PubMed: 10507726]

5. Schouten JP, McElgunn CJ, Waaijer R, Zwijnenburg D, Diepvens F, Pals G. Relative quantification of 40 nucleic acid sequences by multiplex ligation-dependent probe amplification. Nucleic Acids Res 2002;30:E57. [PubMed: 12060695]
6. Vithana EN, Abu-Safieh L, Allen MJ, et al. A human homolog of yeast pre-mRNA splicing gene, *PRP31*, underlies autosomal dominant retinitis pigmentosa on chromosome 19q134 (RP11). Mol Cell 2001;8:375–381. [PubMed: 11545739]
7. Al-Maghtheh M, Vithana E, Tarttelin E, et al. Evidence for a major retinitis pigmentosa locus on 19q13.4 (RP11) and association with a unique bimodal expressivity phenotype. Am J Hum Genet 1996;59:864–871. [PubMed: 8808602]
8. McGee TL, Devoto M, Ott J, Berson EL, Dryja TP. Evidence that the penetrance of mutations at the RP11 locus causing dominant retinitis pigmentosa is influenced by a gene linked to the homologous RP11 allele. Am J Hum Genet 1997;61:1059–1066. [PubMed: 9345108]
9. Vithana EN, Abu-Safieh L, Pelosini L, et al. Expression of *PRPF31* mRNA in patients with autosomal dominant retinitis pigmentosa: a molecular clue for incomplete penetrance? Invest Ophthalmol Vis Sci 2003;44:4204–4209. [PubMed: 14507862]
10. Abu-Safieh L, Vithana EN, Mantel I, et al. A large deletion in the adRP gene *PRPF31*: evidence that haploinsufficiency is the cause of disease. Mol Vis 2006;12:384–388. [PubMed: 16636657]
11. Rivolta C, McGee TL, Frio TR, Jensen RV, Berson EL, Dryja TP. Variation in retinitis pigmentosa-11 (*PRPF31* or RP11) gene expression between symptomatic and asymptomatic patients with dominant RP11 mutations. Hum Mutat. 2006
12. Lathrop GM, Lalouel JM, Julier C, Ott J. Strategies for multilocus linkage analysis in humans. Proc Natl Acad Sci USA 1984;81:3443–3446. [PubMed: 6587361]
13. Stern RF, Roberts RG, Mann K, Yau SC, Berg J, Ogilvie CM. Multiplex ligation-dependent probe amplification using a completely synthetic probe set. BioTechniques 2004;37:399–405. [PubMed: 15470894]
14. White SJ, Breuning MH, den Dunnen JT. Detecting copy number changes in genomic DNA: MAPH and MLPA. Methods Cell Biol 2004;75:751–768. [PubMed: 15603451]
15. Damgaard D, Nissen PH, Jensen LG, et al. Detection of large deletions in the LDL receptor gene with quantitative PCR methods. BMC Med Genet 2005;6:15. [PubMed: 15842735]
16. Deininger PL, Batzer MA. Alu repeats and human disease. Mol Genet Metab 1999;67:183–193. [PubMed: 10381326]
17. Walsh T, Casadei S, Coats KH, et al. Spectrum of mutations in BRCA1, BRCA2, CHEK2, and TP53 in families at high risk of breast cancer. JAMA 2006;295:1379–1388. [PubMed: 16551709]
18. Michils G, Tejpar S, Thoelen R, et al. Large deletions of the APC gene in 15% of mutation-negative patients with classical polyposis (FAP): a Belgian study. Hum Mutat 2005;25:125–134. [PubMed: 15643602]
19. Wang J, Ban MR, Hegele RA. Multiplex ligation-dependent probe amplification of LDLR enhances molecular diagnosis of familial hypercholesterolemia. J Lipid Res 2005;46:366–372. [PubMed: 15576851]
20. Vink GR, White SJ, Gabelic S, Hogendoorn PC, Breuning MH, Bakker E. Mutation screening of EXT1 and EXT2 by direct sequence analysis and MLPA in patients with multiple osteochondromas: splice site mutations and exonic deletions account for more than half of the mutations. Eur J Hum Genet 2005;13:470–474. [PubMed: 15586175]

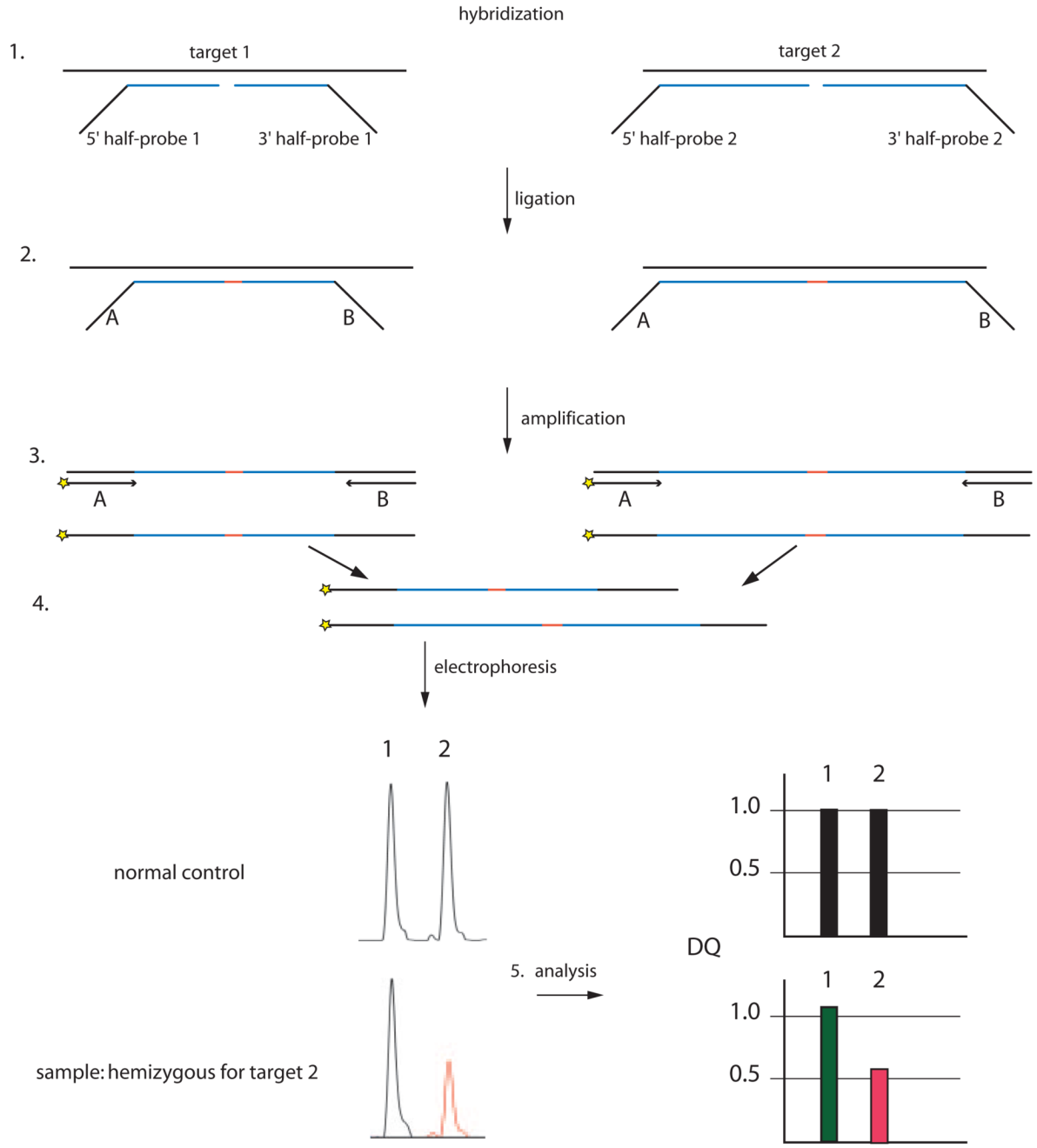

Figure 1.

(**1**) Hybridization of two half-probes to each unique target site in the genome. (**2**) Ligation of each half-probe pair, unless one or both half-probes did not hybridize correctly due to deletion or base mismatches. (**3**) Amplification of each probe with fluorescently labeled universal primers. Amplification products from each target are a unique size. (**4**) Capillary electrophoresis of amplified probes. Areas under each probe peak were calculated and compared to control samples. (**5**) DQs were calculated relative to control samples. A DQ of 1.0 indicates that two alleles are being amplified. DQs <0.6 or greater than 1.4 were investigated further. In this example, probe 1 is normal, whereas probe 2 appears to be hemizygous.

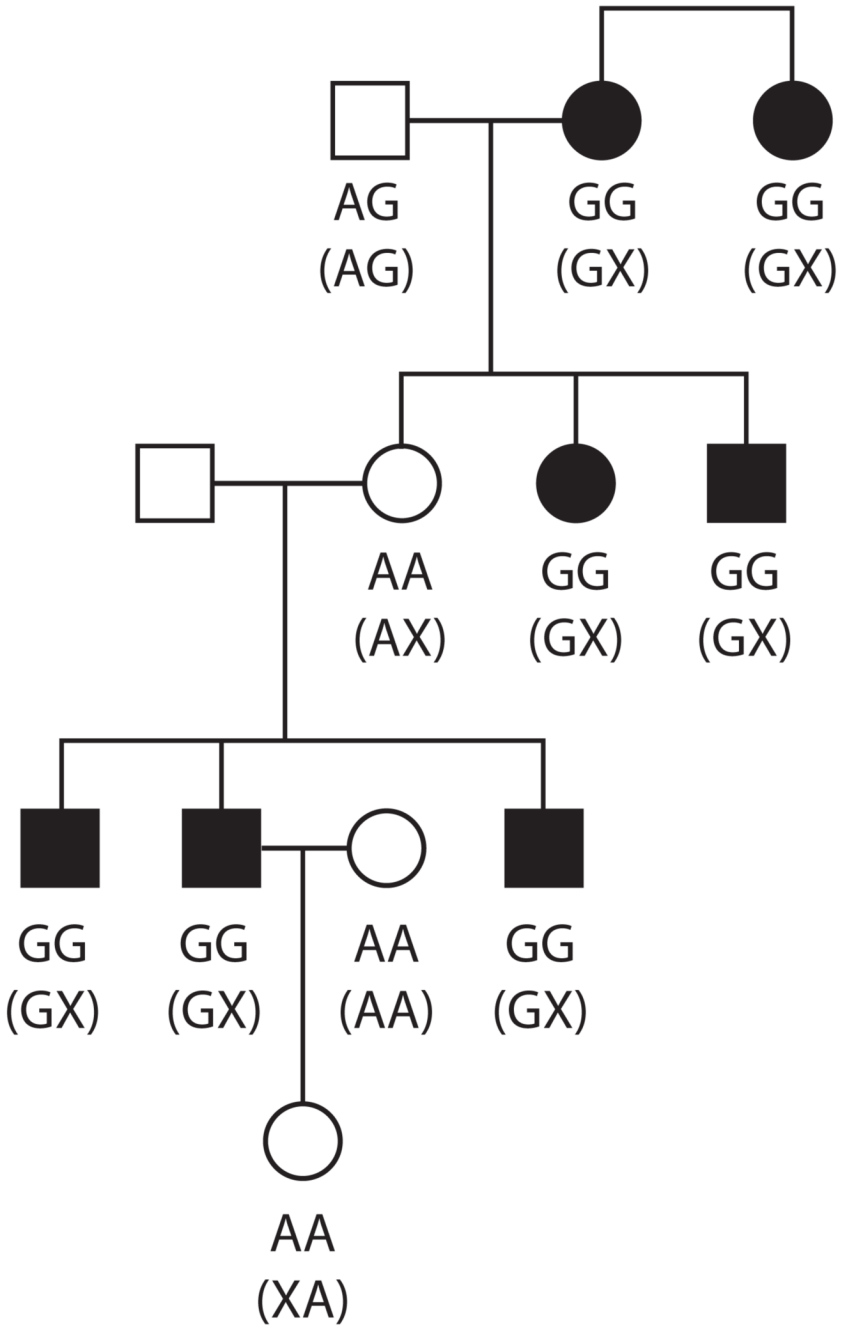

Figure 2.
Abnormal segregation of SNP rs4806711 in BCMAD014. Actual genotypes are shown in parentheses, observed genotypes are shown above. X, the allele carrying the insertion–deletion that no longer contains the SNP. Multiple individuals appeared to be incompatible with their parents but were actually hemizygous for the SNP.

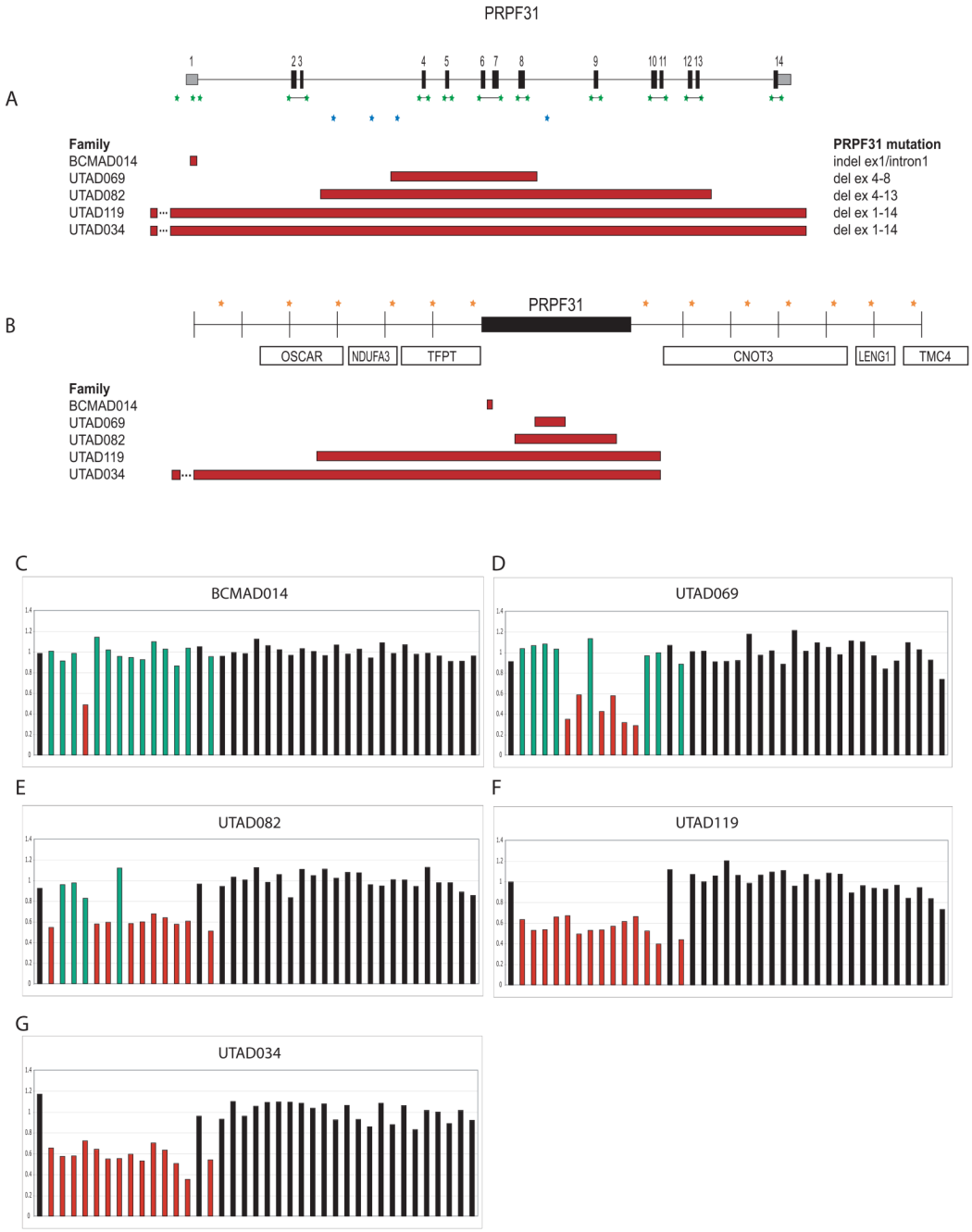

Figure 3.

Mapping of deletions in five families by using MLPA. (**A**) Twenty-one MLPA probes (*green stars*) within the *PRPF31* gene were tested in all families. Four additional internal probes (*blue stars*) were used to refine the deletion breakpoints in UTAD069 and UTAD082. *Red bars*: the extent of each deletion. (**B**) Thirteen flanking probes (*orange stars*) were tested to determine the extent of the deletions in UTAD119 and UTAD034. Probes are spaced at approximate 5-kb intervals on either side of *PRPF31*. The deletion in UTAD034 extends beyond the most 5′ probe tested. (**C**–**G**) Calculated dosage quotients (DQs) for probe set D and control probes from the probe set (P115 Retina; MRC-Holland, Amsterdam, The Netherlands). *Green: PRPF31* probes with normal DQs; *red: PRPF31* probes with abnormal DQs. *Black*:

control probes from the set, including probes for rhodopsin, *RP1*, and *RPE65* as well as other controls.

Table 1

STR Markers Tested in *BCMAD014* for Linkage Exclusion

Ch.adRP Locus	Location (bp)*	Marker	Marker Location (bp)*	LOD Score at $\theta = 0$	z_{max}	θ at z_{max}
1PRPF3	147,110,423–147,138,741	D1S3466	146,997,167	−6.41	0.1	0.15
		D1S498	148,114,569	−∞	0.16	0.25
3RHO	130,730,179–130,736,885	D3S3606	128,682,904	−13.49	0.13	0.3
		D3S1587	132,281,516	−6.1	0.06	0.4
		D3S1292	133,113,007	−13.02	0.07	0.3
6RDS	42,772,317–42,798,287	D6S1549	41,493,345	0.22	0.22	0
		D6S1552	42,063,088	−∞	0.55	0.2
		D6S1582	43,206,595	−∞	1.05	0.1
		D6S282	43,342,553	−6.91	0.84	0.1
7RP9 locus	32,907,651–32,922,242	D7S2252	31,846,821	−13.87	0.1	0.3
		D7S484	35,058,146	−14.46	−0.2	0.4
7IMPDH1	127,626,282–127,644,257	D7S2501	127,106,469	−7.58	0	0.4
		D7S530	128,796,371	−6.97	−0.12	0.4
8RP1	55,691,179–55,705,947	GATA4E08	54,706,451	−∞	0.04	0.3
		D8S1737	54,949,198	−∞	0.09	0.4
		D8S2332	56,292,649	−∞	−0.12	0.4
11ROM1	62,137,198–62,139,162	D11S4191	59,756,135	−∞	0.45	0.15
		D11S987	67,649,917	−∞	0.2	0.3
14NRL	23,619,184–23,623,658	D14S972	23,417,393	−∞	0.09	0.2
		D14S275	25,766,613	−6.72	0.3	0.15
17PRPF8	1,506,434–1,510,872	D17S849	379,287	0.67	0.67	0
		D17S926	576,983	−5.99	−0.01	0.4
		D17S831	1,857,150	0.4	0.4	0
17CA4	55,582,078–55,591,683	D17S957	52,828,496	−∞	−0.05	0.4
		D17S944	58,789,906	−20.93	−0.12	0.4
17FSCN2	77,110,016–77,114,631	D17S784	75,416,716	−6.58	0.31	0.15
		D17S928	77,846,128	−13.33	−0.07	0.4
19CRX	53,016,975–53,038,392	D19S903	49,737,741	−3.56	0.46	0.2
		D19S902	53,023,840	−10.93	−0.08	0.4
19PRPF31	59,310,649–59,326,952	D19S572	58,797,163	−∞	0.65	0.2
		D19S927	58,990,107	1.52	1.52	0
		CA repeat	59,318,821	0.19	0.19	0
		D19S418	60,237,646	1.83	1.83	0
XRPGR	37,884,818–37,942,892	DXS1049	34,936,703	0.21	0.23	0.05
		DXS1068	38,664,206	0.65	0.65	0
		DXS993	40,903,891	0.61	0.61	0
XRP2	46,452,628–46,498,043	DXS1055	46,182,618	−1.54	0.23	0.03
		DXS1039	49,161,528	−∞	−0.02	0.4

*Position on chromosome based on the UCSC human genome assembly of May 2004 (hg17).

Table 2

SNPs Tested in BCMAD014 to Detect Hemizygosity

dbSNP No.	Genomic Location (bp)*	Location within *PRPF31* Gene	Normal Segregation in *BCMAD014*
1rs4806711	59,311,003	IVS1 + 14	No
2rs2668836	59,311,669	IVS1 + 680	Yes
3rs10418693	59,314,300	IVS3 + 475	Yes
4rs12977139	59,314,402	IVS3 + 577	Yes
5rs254278	59,315,588	IVS3 + 1763	Yes
6rs7248976	59,316,238	IVS3 + 2413	Yes
7rs254276	59,317,866	IVS5 + 81	Yes
8rs11670086	59,319,437	IVS7 + 328	Yes
9rs3079638	59,320,701	IVS8 + 854	Yes
10rs254274	59,320,752	IVS8 + 905	Yes
11rs254272	59,321,509	IVS8 + 1662	Yes
12rs8102427	59,322,960	IVS9 + 1156	Yes
13rs171703	59,323,190	IVS9 + 1386	Yes
14rs667324	59,323,748	IVS11 + 184	Yes
15rs2576453	59,324,065	IVS11 + 501	Yes
16rs655240	59,324,235	IVS11 + 671	Yes
17rs11669539	59,325,534	IVS13 + 977	Yes

* Position on chromosome based on the UCSC human genome assembly of May 2004 (hg17).

Table 3

MLPA Probes for PRPF31 and Surrounding Region

Exon	Probe Location*	Size (kb)	Probe Set
PRPF31 screening probes			
Promoter	59310285–59310346	104	X
1	59310844–59310910	108	D
1	59310931–59310997	106	D
2–3	59313356–59313433	114	D
2–3	59313891–59313970	122	X
4	59316988–59317055	110	D
4	59317204–59317273	112	D
5	59317754–59317831	120	D
5	59317630–59317711	124	D
6–7	59318550–59318641	117	D
6–7	59319131–59319207	118	X
8	59319596–59319680	127	X
8	59320039–59320126	130	D
9	59321566–59321656	133	D
9	59321852–59321946	136	D
10–11	59323129–59323187	101	X
10–11	59323624–59323726	145	D
12–13	59324157–59324211	97	X
12–13	59324676–59324732	99	D
14	59326477–59326576	142	X
14	59326712–59326776	104	D
Flanking probes			
Intergenic	59283753–59283840	130	A,B
OSCAR	59290949–59291012	106	B
OSCAR	59295848–59295909	104	A
NDUFA3	59301055–59301113	101	A,B
TFPT	59305253–59305307	97	A,B
TFPT	59309585–59309669	127	A,B
Intergenic	59328550–59328629	122	A,B
CNOT3	59333288–59333353	108	A,B
CNOT3	59338529–59338596	110	A
CNOT3	59343678–59343747	112	B
CNOT3	59348041–59348114	114	A
LENG1	59351374–59351447	116	B
TMC4	59355876–59355951	118	B
Internal breakpoint mapping probes			
PRPF31	59315002–59315092	133	A
PRPF31	59315742–59315835	136	B
PRPF31	59316091–59316187	139	A
PRPF31	59321012–59321111	142	B

* Position on chromosome based on the UCSC human genome assembly of May 2004 (hg17).

Table 4

Summary of Mutations

Family	Mutation Type	Size	Location*
BCMAD014	Insertion/deletion	149 bp deleted/640 bp inserted	Deletion of 59,310,880–59,311,028/insertion of 59,292,594–59,291,955 (reverse comp.)
UTAD069	Deletion	4.8 kb	59,315,842–59,320,684
UTAD082	Deletion	11.3 kb	59,314,340–59,325,633
UTAD119	Deletion	32–42 kb	5′ breakpoint: 59,290,949–59,295,848 3′ breakpoint: 59,328,550–59,333,288
UTAD034	Deletion	>44.8 kb	5′ breakpoint: <59,283,753 3′ breakpoint: 59,328,550–59,333,288

* Position on chromosome based on the UCSC Human Genome Assembly of May 2004 (hg17).